NASA TECHNICAL NOTE

NASA TN D-7603

NASA TN D-7603

A SIMPLIFIED FLIGHT-TEST METHOD FOR DETERMINING AIRCRAFT TAKEOFF PERFORMANCE THAT INCLUDES EFFECTS OF PILOT TECHNIQUE

by Terry J. Larson and William G. Schweikhard

Flight Research Center
Edwards, Calif. 93523

NATIONAL AERONAUTICS AND SPACE ADMINISTRATION • WASHINGTON, D. C. • FEBRUARY 1974

1. Report No.	2. Government Accession No.	3. Recipient's Catalog No.
NASA TN D-7603		

4. Title and Subtitle	5. Report Date
A SIMPLIFIED FLIGHT-TEST METHOD FOR DETERMINING AIRCRAFT TAKEOFF PERFORMANCE THAT INCLUDES EFFECTS OF PILOT TECHNIQUE	February 1974
	6. Performing Organization Code
7. Author(s)	8. Performing Organization Report No.
Terry J. Larson and William G. Schweikhard	H-802
	10. Work Unit No.
9. Performing Organization Name and Address	766-72-02
NASA Flight Research Center P. O. Box 273 Edwards, California 93523	11. Contract or Grant No.
	13. Type of Report and Period Covered
12. Sponsoring Agency Name and Address	Technical Note
National Aeronautics and Space Administration Washington, D. C. 20546	14. Sponsoring Agency Code

15. Supplementary Notes

16. Abstract

A method for evaluating aircraft takeoff performance from brake release to air-phase height that requires fewer tests than conventionally required is evaluated with data for the XB-70 airplane. The method defines the effects of pilot technique on takeoff performance quantitatively, including the decrease in acceleration from drag due to lift. For a given takeoff weight and throttle setting, a single takeoff provides enough data to establish a standardizing relationship for the distance from brake release to any point where velocity is appropriate to rotation. The lower rotation rates penalized takeoff performance in terms of ground roll distance; the lowest observed rotation rate required a ground roll distance that was 19 percent longer than the highest. Rotations at the minimum rate also resulted in lift-off velocities that were approximately 5 knots lower than the highest rotation rate at any given lift-off distance.

17. Key Words (Suggested by Author(s))	18. Distribution Statement
Takeoff performance Aircraft performance test method Evaluating pilot effects on aircraft performance	Unclassified - Unlimited Cat. 02

19. Security Classif. (of this report)	20. Security Classif. (of this page)	21. No. of Pages	22. Price*
Unclassified	Unclassified	39	$3.00

* For sale by the National Technical Information Service, Springfield, Virginia 22151

A SIMPLIFIED FLIGHT-TEST METHOD FOR DETERMINING AIRCRAFT TAKEOFF PERFORMANCE THAT INCLUDES EFFECTS OF PILOT TECHNIQUE

Terry J. Larson and William G. Schweikhard
Flight Research Center

INTRODUCTION

Aircraft takeoff performance must be evaluated to establish the limits of aircraft operation and for certification purposes. It is usually determined by analyzing many separate takeoffs, as in reference 1. With this approach, data for each takeoff are corrected to standard conditions (usually zero wind and sea-level values of thrust, density, and weight) by using the methods outlined in reference 2. The procedure requires a great deal of test support and can also consume considerable time. Furthermore, although much of the scatter in the resulting data is usually attributed to variations in pilot technique, the method does not determine the effects on aircraft performance of different types of variation in pilot input. For example, reference 1 analyzed over 50 takeoffs made by the XB-70 airplane, but the effects of variations in pilot technique on performance could be only inferred. For this reason, test techniques and analytical methods are needed that provide all the information pertinent to the aircraft's performance, including the effects of pilot inputs. A technique that reduces the test effort and the time necessary to produce the data would be especially attractive.

This paper presents a method that determines the takeoff performance of an aircraft, including the effects of pilot technique, from a small number of takeoffs. The method is applied to some of the XB-70 takeoffs reported in reference 1; the takeoff performance of this airplane is especially sensitive to pilot technique. Although the method is applied to this airplane only, it can be applied to any aircraft that takes off horizontally.

SYMBOLS

Physical quantities in this report are given in the International System of Units (SI) and parenthetically in U.S. Customary Units. Measurements were taken in U.S. Customary Units. Factors relating the two systems are presented in reference 3.

A	wing aspect ratio

a aircraft acceleration parallel to runway, m/sec^2 (ft/sec^2)

C_D aerodynamic drag coefficient

C_{D_i} induced drag coefficient

C_{D_0} zero-lift drag coefficient

C_L aerodynamic lift coefficient

D average aerodynamic drag, N (lbf)

E energy, joules (ft-lbf)

$e = \dfrac{\dfrac{dC_{D_i}}{dC_L^2}}{\dfrac{dC_D}{dC_L^2}}$, Oswald efficiency factor

F_g average gross thrust of aircraft during ground roll or air phase, N (lbf)

F_n average net thrust of aircraft during ground roll or air phase, N (lbf)

g acceleration due to gravity, m/sec^2 (ft/sec^2)

h geometric height above runway, m (ft)

h_a air-phase height, m (ft)

$h_v = \dfrac{V_a^2 - V_{lof}^2}{2g}$, specific airplane kinetic energy increase during air phase, m (ft)

$K = \left(\dfrac{W_s}{W_t}\right)\left(\dfrac{\rho_t}{\rho_s}\right)\left(\dfrac{V_{r_t}}{V_{r_s}}\right)^2$, correction factor for applying equations that define ΔV_{r_a} and ΔS_{r_a} for standard conditions to test conditions

k intercept of straight line

m slope of straight line

S	wing area, m^2 (ft^2)
S_a	air-phase distance, horizontal distance traveled by aircraft from lift-off to air-phase height, m (ft)
S_g	ground roll distance traveled by aircraft from brake release to lift-off, m (ft)
S_h	distance from lift-off to height, h, above runway during air phase, m (ft)
S_r	ground roll distance traveled by aircraft from brake release to initiation of rotation, m (ft)
$S_{r_{s(V)}}$	ground roll distance traveled by aircraft from brake release to initiation of rotation, standardized for relating distance to aircraft velocity, m (ft)
t	time, sec
V	aircraft velocity, knots or m/sec (ft/sec)
V_a	velocity at air-phase height, knots or m/sec (ft/sec)
W	aircraft weight, kN (lbf)
α	aircraft angle of attack, deg
$\dot{\alpha} = \frac{\alpha_{lof} - \alpha_r}{\Delta t_r}$, deg/sec	
Δ	algebraic change in value of reference variable
ΔS_r	distance from beginning of rotation to lift-off, m (ft)
ΔS_{r_a}	change in horizontal distance during rotation due to the deviation of acceleration from initial value (negative value represents loss of distance), m (ft)
Δt_r	time from beginning of rotation to lift-off, sec
ΔV_r	change in velocity from beginning of rotation to lift-off, knots or m/sec (ft/sec)
ΔV_{r_a}	change in velocity during rotation due to the deviation of acceleration from initial value (negative value represents loss in velocity), knots or m/sec (ft/sec)
μ	coefficient of rolling friction

ρ	ambient density, kg/m^3 ($slugs/ft^3$)
σ	ratio of measured ambient density to standard sea-level value

Subscripts:

eff	effective, referenced to time during rotation phase when decrease in acceleration becomes significant
lof	referenced to time of aircraft lift-off
p_1	calculated value based on lift curve in ground effect
p_2	value based on takeoff measurements of the variation of $\frac{\partial a}{\partial \alpha}$ with α
r	referenced to time of initiation of rotation
s	standardized value
t	test or measured value

AIRCRAFT DESCRIPTION

The XB-70 airplane used in this investigation (fig. 1) was a large, delta-winged aircraft designed for long-range supersonic cruise. The airplane was designed to cruise at a Mach number of 3 and to take off at weights of more than 2224 kilonewtons (500,000 pounds force). Data for the two XB-70 aircraft are presented; their configurations are described in detail in reference 4, and information pertaining to takeoff configuration and operating procedure is given in reference 1.

DATA SOURCE AND ACCURACY

The data in this paper are from some of the takeoffs reported in reference 1. Instrumentation and data processing were as described in that report. Angle of attack was measured from a vane mounted on a nose boom, and fuel quantity, which was measured for weight determination, was recorded by a pulse-code-modulation system. Optical space-positioning measurements were obtained from a cinetheodolite tracking system, and meteorological information was provided by the Air Weather Service at Edwards Air Force Base.

Runs were selected according to the normalcy of the pilot's takeoff techniques, the accuracy of the space-positioning data, and the degree of correction necessary to standardize the distances and velocities.

The standardization procedures are described in appendix A of reference 1. The accuracy of basic measurements is repeated below for convenience.

Position	±0.6 m (±2 ft)
Velocity	±1 knot
Acceleration	±0.03 m/sec^2 (±0.1 ft/sec^2)
Angle of attack	±0.5°
Thrust	±22 kN (±5000 lbf)
Weight	±2.22 kN (±500 lbf)
Temperature	±0.6° C (±1° F)
Pressure	±100 N/m^2 (±2 lbf/ft^2)

TAKEOFF PERFORMANCE

General Procedure

Takeoffs are usually thought of as having two phases (see fig. 2), a ground roll phase (from brake release to the lift-off of the last aircraft wheel) and an air phase (from lift-off to an arbitrary height sometimes called barrier height and referred to herein as air-phase height). In this paper, the sum of the ground roll and air-phase distances is termed the field length.

For the proposed method, the ground roll phase is divided into two parts, one from brake release to the beginning of aircraft rotation, the second from rotation to lift-off. If throttling procedures do not vary significantly from one takeoff to the next, the effects of pilot technique on performance are confined to the relatively short rotation phase.

Assuming that pilot technique effects are absent before aircraft rotation, for a given weight and under standard atmospheric and aircraft conditions the distance from brake release to rotation is a single-valued function of velocity. Therefore, this relationship can be established for any standardized aircraft weight with only one takeoff. A plot of this relationship can be used to determine the distance from brake release to the initiation of rotation.

Aircraft ground roll performance is affected by the forward velocity at which the pilot begins to rotate the aircraft and the way in which he performs the rotation. Further, if drag due to lift is large, as it is for the XB-70 airplane, lift-off velocity and distance cannot be accurately defined by a single standardized curve, because acceleration during the rotation decreases in a manner that depends on the pilot's rotation technique.

The proposed method allows the change in distance and velocity from the beginning of rotation to lift-off to be determined for a given rotation starting velocity and rotation rate. Therefore velocity and distance at lift-off can be determined by adding these increments to the velocity and distance at rotation.

For conventional evaluations of air-phase performance, the gain in specific energy from lift-off to the air-phase height is determined. Many takeoffs are necessary to establish the relationship between specific energy and air-phase distance (distance from lift-off to air-phase height). Once established, this relationship defines velocity at the air-phase height.

The proposed method for determining air-phase performance is similar to that proposed for the prerotation phase. That is, a series of data points obtained from one takeoff is used to determine specific energy gain as a function of distance instead of a set of points obtained one by one in a series of takeoffs for the air-phase height.

The following sections describe the method in detail for each phase of takeoff. Appendix A outlines the procedures for the general application of the method.

Ground Roll Prior to Rotation

Reference 1 presents data for velocity at initiation of rotation plotted against distance from brake release for three aircraft weights. For reference purposes, data from that paper for a standard weight of 2313 kilonewtons (520,000 pounds force) are shown in figure 3. Each data point in figure 3 represents a single ground roll test. The distances are standardized for weight, density, and thrust, and the velocities are standardized for lift coefficient.

Because the effects of pilot technique are confined to the rotation phase, the ground roll distance traveled by an airplane from brake release to initiation of rotation is a single-valued function of aircraft velocity for a given aircraft weight under standard conditions. Hence, a sequence of data points from only one takeoff can be used to establish this relationship. Each point can be standardized as described in reference 1. These points can then be considered to correspond with the time of rotation, and a plot using the same abscissa and ordinate as figure 3 can be constructed. A fairing of these points should give essentially the same results as the data obtained conventionally, as in figure 3. Hence, for a given weight, only one takeoff is necessary to define the ground roll distance for any velocity appropriate to initiation of rotation.

Rotation

Change in acceleration, velocity, and distance during rotation. — Variations in the pilot's rotation technique are reflected in time histories of aircraft acceleration during rotation. Figure 4 shows a time history of the acceleration and angle of attack of the XB-70 airplane during a typical rotation. For purposes of comparison, a time history of acceleration calculated from wind-tunnel data from reference 5 is included. The equation used for the calculation, which results from summing the

forces and accelerations along the ground track, is as follows:

$$a = \frac{1}{\frac{W}{g}}\left[F_n \cos\alpha + \mu\left(0.5\rho V^2 S C_L - W\right) - 0.5\rho V^2 S\left(\frac{C_L^2}{\pi Ae} + C_{D_0}\right)\right] \qquad (1)$$

Values of C_L and C_{D_0} were taken from reference 5 as a function of the measured angle of attack. The acceleration curves are similar in shape, and the increase in the measured angle of attack is nearly linear during most of the rotation.

The loss of acceleration during rotation that is apparent in figure 4 is primarily due to a large increase in drag due to lift, which is typical of delta-winged aircraft. Figure 5 shows the change in acceleration calculated for a constant rate of angle-of-attack change for the XB-70 airplane. The change due to induced drag is much larger than that due to ground rolling friction or thrust.

If acceleration during rotation were constant, the changes in velocity and distance during rotation would be easy to determine, provided that this acceleration and the time taken to rotate, Δt_r, could be determined experimentally. With a loss of acceleration during rotation, however, velocity and distance at lift-off are less for a given Δt_r than for constant acceleration. If the losses in velocity and distance at lift-off due to decreasing acceleration during rotation are referred to as ΔV_{r_a} and ΔS_{r_a}, ΔV_r and ΔS_r can be written as follows:

$$\Delta V_r = V_{lof} - V_r = a_r \Delta t_r + \Delta V_{r_a} \qquad (2)$$

$$\Delta S_r = S_g - S_r = \frac{a_r}{2}\left(\Delta t_r\right)^2 + V_r \Delta t_r + \Delta S_{r_a} \qquad (3)$$

The components of ΔV_r and ΔS_r are shown in figure 6, along with other terms pertaining to rotation.

From equations (2) and (3), it is apparent that to determine ΔV_r and ΔS_r from given values of V_r and S_r the quantities a_r, Δt_r, ΔV_{r_a}, and ΔS_{r_a} must be determined. These quantities can be approximated by simple linear functional relationships involving only basic aircraft and atmospheric quantities that usually can be considered constant for a given rotation.

Determination of a_r and Δt_r. — For the period between brake release and the beginning of rotation, acceleration is a function of thrust, weight, and velocity for given runway conditions. For jet aircraft like the XB-70 airplane, acceleration is nearly constant during this period, and acceleration at rotation is about equal to the thrust-to-weight ratio. Hence, plotting the acceleration measured at rotation

during one or two tests as a function of $\frac{F_n}{W_t}$ (or $\frac{F_g}{W_t}$, if thrust values are available only from the engine manufacturer's specifications) allows a_r to be determined for other thrust-to-weight ratios; that is,

$$a_{r_t} = \left(\frac{F_{g_t}}{F_{g_s}}\right)\left(\frac{W_s}{W_t}\right)a_{r_s} \tag{4}$$

A method for determining a_r when acceleration is a function of velocity is described in appendix B.

The time it takes to rotate, Δt_r, is a linear function of known quantities, assuming that (1) the rate of change of angle of attack is constant (or that an average rate computed for a given rotation in which $\dot{\alpha}$ varies is an adequate approximation), (2) lift equals weight at lift-off, and (3) the lift-curve slope is linear. First writing

$$C_{L_{lof}} = C_{L_r} + \dot{\alpha}\Delta t_r \frac{\partial C_L}{\partial \alpha} \tag{5}$$

and solving for Δt_r results in

$$\Delta t_r = \frac{C_{L_{lof}} - C_{L_r}}{\dot{\alpha}\frac{\partial C_L}{\partial \alpha}} \tag{6}$$

Thus, Δt_r is proportional to $\frac{C_{L_{lof}}}{\dot{\alpha}}$. But because $C_{L_{lof}}$ equals $\frac{W}{0.5\rho(V_{lof}^2)S}$, it follows that

$$\Delta t_r : \frac{W}{\sigma(V_{lof})^2\dot{\alpha}} \tag{7}$$

Determination of ΔV_{r_a} and ΔS_{r_a}. — To evaluate the changes in velocity and distance that result from the decrease of acceleration during rotation, the variation of acceleration during rotation must be determined.

For a delta-winged aircraft, the variable that most affects acceleration during rotation is C_L. Therefore the differential $\frac{da}{dt}$ can be approximated by the

equation

$$\frac{da}{dt} \approx \frac{\partial a}{\partial C_L} \frac{dC_L}{dt} \tag{8}$$

This equation is valid except at small angles of attack, where the order of magnitude of the rolling friction approaches that of the induced drag and the loss of acceleration is small (see fig. 5).

The quantity $\frac{\partial a}{\partial C_L}$ in equation (8) can be derived by differentiating equation (1):

$$\frac{\partial a}{\partial C_L} = \frac{\rho V^2 S g}{2W} \left(\mu - \frac{2C_L}{\pi A e} \right) \tag{9}$$

Hence, if the lift curve is known in ground effect (C_L as a function of α), $\frac{da}{dt}$ can be evaluated for a given variation of C_L or angle of attack during rotation. This calculation method, referred to herein as the p_1 method, is compared with the test, or p_2, method in the RESULTS AND DISCUSSION section.

When the test method is used, the lift curve need not be known, but it is assumed that C_L is linear with α during rotation. This allows the variables to be transformed so that equation (8) can be written as follows:

$$\frac{da}{dt} \approx \left(\frac{\partial a}{\partial \alpha} \right) \dot{\alpha} \tag{10}$$

If $\frac{\partial a}{\partial C_L}$ varies linearly with C_L, as indicated by equation (9), $\frac{\partial a}{\partial \alpha}$ is also linear with α and can be determined with a minimum amount of testing. If this relationship and the given rotation rate (or the variation of angle of attack with time during rotation) are known, equation (10) can be used to determine $\frac{da}{dt}$. The assumption that $\frac{\partial a}{\partial C_L}$ is linear with C_L is reasonable, provided that the effect of the change in velocity during rotation is small compared to the variation in C_L (eq. (9)).

The experimental relationship of acceleration to angle of attack can be standardized by the relationship shown in equation (11).

$$\left(\frac{\partial a}{\partial \alpha}\right)_s = \frac{\left(\frac{\rho V_r^2}{W}\right)_s}{\left(\frac{\rho V_r^2}{W}\right)_t}\left(\frac{\partial a}{\partial \alpha}\right)_t \tag{11}$$

which results directly from equation (9). Once $\left(\frac{\partial a}{\partial \alpha}\right)_s$ is defined, $\left(\frac{\partial a}{\partial \alpha}\right)_t$ can be determined for test conditions of ρ, V_r, and W.

The variation of acceleration at the low angles of attack that occur early in rotation depends on rolling friction as well as C_L. Therefore $\frac{\partial a}{\partial \alpha}$ does not vary linearly at low angles of attack. Rotation rate is not linear early in rotation either, because it takes a certain amount of time for the rotation rate to increase from zero to the average rotation rate (see fig. 6). However, the change in acceleration during this period is ordinarily small and has little effect on ΔV_{r_a} or ΔS_{r_a}. Therefore $\frac{da}{dt}$ need be evaluated only in the rotation phase corresponding to higher angles of attack, where the loss of acceleration is important and $\frac{\partial a}{\partial \alpha}$ is nearly linear with α. An integral equation for acceleration then follows from equation (10):

$$a = \int_0^{\Delta t_{r_{eff}}} \left(\frac{\partial a}{\partial \alpha}\right)\dot{\alpha}\, dt + a_r \tag{12}$$

where $\Delta t_{r_{eff}}$ is the effective rotation time given by $t_{lof} - t_{r_{eff}}$. The time $t_{r_{eff}}$ is defined as the time when the change in acceleration after initiation of rotation becomes significant, and it can be identified in terms of angle of attack.

Appendix C gives general derivations of $\left(\Delta V_{r_a}\right)_{p_2}$ and $\left(\Delta S_{r_a}\right)_{p_2}$ from the definition of $\left(\frac{da}{d\alpha}\right)_t$. Another way to define ΔV_{r_a} and ΔS_{r_a} is to plot test values of acceleration as a function of α^2 instead of $\frac{da}{d\alpha}$ as a function of α. Both plots result in linear relationships.

Air Phase

The conventional way to determine specific kinetic energy gain is to subtract the level of kinetic energy at lift-off from that at a particular height (air-phase height). This is the method used in reference 1. In the test method, total specific energy (the sum of kinetic and potential energy gains) is calculated at many points in the climbout.

In equation form, the specific energy gain at a given point during climbout is

$$\Delta\frac{E}{W} = h + \frac{V^2 - V_{lof}^2}{2g} \tag{13}$$

Specific energy gain can also be written

$$\Delta\frac{E}{W} = \left(\frac{F_n - D}{W}\right)S_h \tag{14}$$

where S_h is the distance from lift-off to height, h. Combining equations (13) and (14) results in

$$S_h = \left(\frac{W}{F_n - D}\right)\left(h + \frac{V^2 - V_{lof}^2}{2g}\right) \tag{15}$$

Therefore, for a given value of $\frac{W}{F_n - D}$, the distance from lift-off is a linear function of the sums of the specific potential and kinetic energy gains.

With the proposed single takeoff method, distances from lift-off are standardized by using the technique used to standardize air-phase distance in reference 1. The distances from lift-off are then plotted as a function of $\Delta\frac{E}{W}$. Because $h_v = \Delta\frac{E}{W} - h_a$, the curve generated by these points is displaced from the curve generated with the conventional method by the air-phase height.

RESULTS AND DISCUSSION

Evaluation of Proposed Method

Ground roll prior to rotation. — Figure 7 compares the variation of ground roll distance with velocity at rotation for the conventional and single takeoff methods. Data derived by the single takeoff method are shown for two ground roll tests, one for each XB-70 airplane. Each point was standardized in the same way as for

the reference 1 data. The agreement between the two sets of ground roll data from the single takeoff method is excellent. Differences between the data from these tests are well within the scatter of the data determined by conventional means (fig. 3).

The data from the single takeoff method also agree well with a fairing of the data from reference 1. Thus, for a given aircraft weight and throttle setting, a single takeoff provided enough data to establish a standardizing relationship that indicates the ground roll distance from brake release to any point where velocity is appropriate to the initiation of rotation.

Rotation. — Figure 8 presents data for acceleration at rotation as a function of $\left(\frac{F_{g_t}}{F_{g_s}}\right)\left(\frac{W_s}{W_t}\right)$ for individual flights. According to the scatter in this figure, a linear fairing of a_r is accurate to ±0.06 m/sec^2 (±0.2 ft/sec^2).

In figure 9, Δt_r is plotted as a function of $\frac{W_t}{\sigma V_{lof}^2 \dot{\alpha}}$ for individual flights. With a linear fairing of the data, Δt_r can be determined with an accuracy of approximately 0.5 second. It was estimated that half of the scatter was due to measurement errors in Δt_r. The linear curve in figure 9 indicates that an assumption of constant angle-of-attack rate during rotation is acceptable for this analysis.

The data in figure 4 were used to determine the variation of $\frac{\partial a}{\partial \alpha}$ with angle of attack. As shown in figure 10, points were calculated for every half degree from 3° to 7.5°. A straight line was drawn through the data between 4° and 6.5° and linearly extrapolated to higher angles of attack. The deviation of the data from linearity at the higher angles of attack is partly due to the effects of velocity on acceleration during rotation. The nonlinearity of the data for $\alpha < 4°$ was expected because of the effects of friction. A value of 4° was used for $\alpha_{r_{eff}}$ since acceleration changed only 0.1 m/sec^2 (0.3 ft/sec^2) before the airplane reached this angle of attack.

The test curve in figure 10 was standardized by using equation (11) and values of W_s equal to 2313 kilonewtons (520,000 pounds force), V_{r_s} equal to 189 knots, and ρ_s equal to 1.2250 kg/m^3 (0.00238 slug/ft^3). The test curve from figure 10 is shown in figure 11 along with this standardized curve and a curve standardized by using equation (9) and wind-tunnel data from reference 5. The standardized curve calculated from wind-tunnel data predicts a smaller loss of acceleration during rotation than the standardized curve calculated from data in figure 10. However, the difference between the two standardized curves, which is less than 0.06 m/sec^2-deg (0.2 ft/sec^2-deg) for any angle of attack, results in a difference of only 1 knot or so in ΔV_{r_a} for typical rotations.

Figure 12 compares calculated and directly measured values of ΔV_{r_a} and ΔS_{r_a} (see appendix D for the calculation procedure). The ΔV_{r_a} values derived by the p_2 method, which are based on takeoff acceleration data, are slightly more accurate than the values derived by the p_1 method, which are based on wind-tunnel data. The values for the p_2 method have a root-mean-square deviation of less than 1 knot from the measured data. As can be inferred from figure 11, the values determined by the p_1 method are, on the average, slightly less than the measured values. Both methods are satisfactory, however, in view of the fact that the loss in velocity during rotation due to decreasing acceleration varies from 2 to 11 knots.

The scatter in the ΔS_{r_a} data is greater than in the ΔV_{r_a} data, but this is not of much significance, because ΔS_{r_a} is small compared with the total change in distance during rotation.

To test the accuracy with which the p_2 method determined ΔV_r and ΔS_r (the total change in velocity and distance during rotation), calculated values of these quantities were also compared with direct measurements. The calculation procedure is outlined in appendix D.

The results are shown in figure 13. The standard deviation between the calculated and measured velocities is less than 2 knots, and that between the calculated and measured distances is approximately 35 meters (115 feet). A large proportion of the difference can be attributed to uncertainty in the measurement of Δt_r. Hence, the changes in velocity and distance during rotation determined with the test method by using pilot-controlled quantities of velocity at the beginning of rotation and rotation rate can be considered to be accurate.

Air phase. — In figure 14, data for $h_v = \Delta \frac{E}{W} - 10.7$ meters (35 feet) as determined from a single takeoff at a standard weight of 2313 kilonewtons (520,000 pounds force) are plotted as a function of standardized air-phase distance. Also shown, from reference 1 and for the same weight, are an analytically predicted curve and data for multiple takeoffs.

The single takeoff data and the analytical curve agree well throughout the air-phase performance range shown. The angle of attack during the single takeoff was close to the 10.5° angle of attack used in the analytical computation. The disagreement between the single takeoff curve and the multiple takeoff data at distances below 600 meters (2000 feet) is believed to be a result of the fact that the angle of attack during the multiple takeoffs was higher than average during the early part of the air phase. As explained in reference 1, the higher the angle of attack, the greater the air-phase distance for a given specific energy gain because of increased drag.

The difference between the two sets of experimental data in figure 14 suggests that the data should be standardized for C_L. As mentioned in reference 1, attempts to standardize for C_L using the conventional technique have not been successful. To define the effects of C_L on air-phase performance with the proposed test method, several takeoffs at different angles of attack would be required.

Effect of Pilot Technique on Takeoff Performance

The test method makes possible a quantitative assessment of the effects of pilot technique on takeoff velocity and distance. It is assumed that the only variables dependent on pilot technique that significantly affect ground roll performance are the velocity at which the rotation is begun, V_r, and the average rotation rate, $\dot{\alpha}$. In the air phase, airplane performance is dependent on energy management.

Figure 15 shows the effect of V_r and $\dot{\alpha}$ on standardized aircraft distance and velocity increments during rotation. For the range of $\dot{\alpha}$ in these data (from 1.2 degrees per second to 3.9 degrees per second), variations of approximately 500 meters (1600 feet) and 25 knots occurred in ΔS_{r_s} and ΔV_{r_s}, respectively. For rotation initiation velocities of 166 knots and 178 knots, rotation rates were limited to 2.5 degrees per second and 3.0 degrees per second, respectively, to keep the angle of attack at lift-off from exceeding 13° (the tail-scraping angle of the XB-70 airplane was 14°).

Figure 15 was used to construct curves showing the relationship of velocity to distance at lift-off. Various values of V_r and S_r at rotation (from fig. 7) were added to corresponding values of ΔV_r and ΔS_r (from fig. 15). Figure 16(a) shows curves constructed in this manner for a weight of 2313 kilonewtons (520,000 pounds force). Lift-off data from reference 1 are presented for comparison with the calculated lift-off curves, which are for $\dot{\alpha}$ values of 1 degree per second, 2 degrees per second, and 4 degrees per second. The displacement of the curves from the rotation curve is due to the loss of acceleration during rotation. The calculated curves explain some of the scatter in the data, which, as noted, were for values of $\dot{\alpha}$ that varied from 1.2 degrees per second to 3.9 degrees per second.

Figures 15 and 16(a) show that the lowest rate of rotation penalized takeoff performance by requiring ground roll distances that were as much as 19 percent longer than the distances for the highest rate. The lowest rate also resulted in lift-off velocities that were as much as 5 knots lower than the highest rotation rate at any given lift-off distance. The lower rotation rates were also undesirable because they tended to reduce the pilot's control over lift-off velocity and attitude. On the other hand, rotation rates that are too high can result in tail scraping. In addition, if the rate of rotation is too high early in rotation, the pilot must reduce it, which causes the aircraft to be at a high angle of attack for a considerable length of time before lift-off. As discussed in reference 6, the time spent in this high drag condition can cause the ground roll to be longer than for a slower rotation. The average rotation

rate reported in reference 1 for the XB-70 airplane was 2.2 degrees per second, and this represents a good compromise between adequate pilot control and optimum ground roll performance.

The three field length curves in figure 16(b) represent conditions of minimum performance, nominal performance, and maximum performance (minimum distance for a given V_{a_s}). Data from reference 1 are also presented. The curves were calculated by adding air-phase distance from the curve in figure 14 to lift-off distances from the curves in figure 16(a). The maximum performance curve ($h_v = 0$ and $\dot{\alpha} = 4$ degrees per second) represents a rotation at the maximum rate assumed to be allowable and a steep constant-velocity takeoff that results in no increase in kinetic energy during the air phase. The minimum distances shown by this curve are based on an angle of attack that is lower than steep climbouts require. The flight data are well represented by the middle curve, which is based on values of h_v and $\dot{\alpha}$ that are close to the average values for the flight data.

CONCLUDING REMARKS

A method for evaluating aircraft takeoff performance that requires fewer takeoffs than the conventional method was investigated. The method was evaluated with the data used for a conventional takeoff performance analysis of the XB-70 airplane. The method makes possible a quantitative assessment of the effects of pilot technique during aircraft rotation that includes the decrease of acceleration from drag due to lift.

For a given aircraft weight and throttle setting, a single takeoff provides enough data to establish a standardizing relationship that indicates the distance from brake release to any point where velocity is appropriate to the initiation of rotation. The method uses the velocity at the beginning of rotation and rotation rate to determine the change in velocity and distance during the rotation phase of the takeoff. The lower rotation rates penalized takeoff performance in terms of ground roll distance; with the lowest observed rotation rate, 1.2 degrees per second, the XB-70 airplane required a ground roll distance that was 19 percent longer than with the highest rotation rate, 3.9 degrees per second. The lowest rate also resulted in lift-off velocities that were as much as 5 knots lower than the highest rotation rate at any given lift-off distance. The average rotation rate used in the takeoffs, 2.2 degrees per second, represented a good compromise between adequate pilot control and optimum ground roll performance.

Flight Research Center
National Aeronautics and Space Administration
Edwards, Calif., Jan. 2, 1974

APPENDIX A

APPLICATION OF TAKEOFF PERFORMANCE TEST METHOD

Takeoff Tests

Although ground roll performance, including the effects of pilot rotation technique, can be determined for a given standard weight and throttle setting from only one takeoff, it is advisable to have at least two takeoffs performed. In addition, at least two tests are necessary to define the effect of angle of attack on the airplane's air-phase performance. The takeoffs should be made at nearly the same weight and within a few percent of the selected standard weight. Winds should be no higher than 5 to 10 knots, and other atmospheric conditions should be near standard day values.

One takeoff should incorporate a slow constant-rate rotation and a steep climbout during the air phase, and the other a rapid constant-rate rotation and a shallow climbout. Rotation should come early in the test of the first type and late in that of the second. Rotation speeds should not be so low that tail scraping is likely or so high that the limit speeds are exceeded, and they should be compatible with flight safety during the subsequent climbouts.

The recommended procedure for standardizing performance quantities from two or more takeoffs performed in the manner just described is outlined below. The relationship of velocity and distance at lift-off to velocity at the beginning of rotation and rotation rate can be determined from these results.

Ground Roll Performance Up to Rotation

First, standardize velocity and distance data for regular intervals during the ground rolls up to rotation by using the standardization procedures described in appendix A of reference 1 to obtain S_{r_s} and $V_{r_{s(V)}}$.

Plot and fair S_{r_s} as a function of $V_{r_{s(V)}}$ for the times selected above. If standardization procedures are adequate, a single curve can be generated from the two sets of data.

Rotation Performance

Calculate the parameter $\left(\frac{F_{g_t}}{F_{g_s}}\right)\left(\frac{W_s}{W_t}\right)$ for each test for the conditions at initiation of rotation. If thrust was not measured, use engine manufacturer specifications. Plot the thrust and weight parameter as a function of acceleration at the beginning

of rotation, a_r. Fair a straight line through the data and the origin of the coordinate system.

Determine Δt_r for each test and plot it as a function of $\frac{W_t}{\sigma V_{lof}^2 \dot{\alpha}}$. Draw a straight line through the two points and extrapolate if necessary. This line should also pass through the origin.

Plot time histories of acceleration and angle of attack for both tests. Calculate $\frac{\partial a}{\partial \alpha}$ and plot it as a function of angle of attack. Define $\alpha_{r_{eff}}$ from the plot as from figure 10. Fair a straight line through each set of data and determine equations for $\frac{\partial a}{\partial \alpha}$ (eq. (C2)). Standardize the equations for the two tests: They should be identical. If they differ significantly, decide whether to standardize the equation on the basis of the average of the test results, to use data for the test considered more accurate, or to perform additional rotations. Develop the equations as described in appendix C to define ΔV_{r_a} and ΔS_{r_a} for standardized conditions.

Air-Phase Performance

Standardize air-phase distance at regular intervals for the two tests by using the equation from appendix A of reference 1 that results in S_{a_s}. Select a standard weight as for a ground roll performance calculation. For each point, calculate the specific energy gained from lift-off, $\Delta \frac{E}{W}$.

Plot and fair S_{a_s} as a function of $\Delta \frac{E}{W}$ or $h_v = \Delta \frac{E}{W} - h_a$. A plot of angle of attack as a function of S_{a_s} is also helpful in interpreting the data. Significant differences between the two sets of data may be due to inaccurate standardization or to differences in drag caused by differences in angle of attack. If the standardization appears to be accurate, the difference is probably due to differences in angle of attack. Additional tests may be warranted to resolve such problems.

APPENDIX B

GENERAL METHOD FOR DETERMINING a_r

When acceleration during ground roll is a function of velocity as well as thrust and weight, an expression for the acceleration at the beginning of rotation can be determined from a plot of acceleration as a function of velocity. Such a plot is typically linear, like that shown in the sketch below for two different takeoffs.

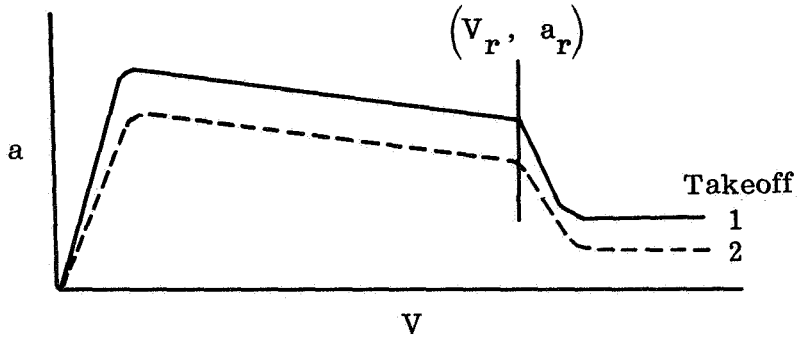

If acceleration is not linear with velocity, it may be necessary to plot acceleration as a function of V^2 or $V^{1/2}$ to achieve a reasonably linear curve.

Assuming, for example, a linear relationship with velocity, a reasonable approximation for acceleration at rotation is

$$a_r = \frac{F_g}{W} + mV_r \tag{B1}$$

where m is the slope of the linear portion of the curve.

The standard day value of acceleration may be derived as follows:

$$\frac{a_s}{a_t} = \frac{\frac{F_{g_s}}{W_s} - mV_r}{\frac{F_{g_t}}{W_t} - mV_r} = \frac{\frac{F_{g_s}}{W_s}}{\frac{F_{g_t}}{W_t} - mV_r} - \frac{mV_r}{\frac{F_{g_t}}{W_t} - mV_r} \tag{B2}$$

The quantity mV_r is usually of the order of one-tenth of $\frac{F_g}{W}$, so the second

term can be dropped for all practical purposes. The standard day acceleration then becomes

$$a_s = \frac{\frac{F_{g_s}}{W_s}}{\frac{F_{g_t}}{W_t} - mV_r} a_t \tag{B3}$$

Reduced, this expression assumes the form presented in the text when the acceleration is not a function of V_r.

APPENDIX C

DERIVATION OF $\left(\Delta V_{r_a}\right)_{p_2}$ AND $\left(\Delta S_{r_a}\right)_{p_2}$

The quantities $\left(\Delta V_{r_a}\right)_{p_2}$ and $\left(\Delta S_{r_a}\right)_{p_2}$ can be determined from the successive integration of the equation

$$\frac{da}{dt} = \frac{\partial a}{\partial \alpha}\dot{\alpha} \tag{C1}$$

In this equation, $\frac{\partial a}{\partial \alpha}$ can be approximated by a linear function of angle of attack and can be defined by one rotation to lift-off (for example, see figs. 4 and 10). Hence, $\frac{\partial a}{\partial \alpha}$ can be written

$$\frac{\partial a}{\partial \alpha} = k + m\alpha \tag{C2}$$

Once this relationship is established for one set of test conditions, it can be standardized for other conditions by using equation (11). Conversely, if the standardized equation is known, equation (11) can be used to calculate an expression for any test condition. That is, if $\left(\frac{\partial a}{\partial \alpha}\right)_s$ has been defined in such a manner, $\left(\frac{\partial a}{\partial \alpha}\right)_t$ can be found because

$$\left(\frac{\partial a}{\partial \alpha}\right)_t = K(k + m\alpha)_s \tag{C3}$$

where

$$K = \left(\frac{W_s}{W_t}\right)\left(\frac{\rho_t}{\rho_s}\right)\left(\frac{V_{r_t}}{V_{r_s}}\right)^2 \tag{C4}$$

which follows from equation (11).

As explained in the text, the variation of acceleration during rotation is important only when the angle of attack reaches an appreciable angle, $\alpha_{r_{eff}}$. Angles of attack that occur after $\alpha_{r_{eff}}$ is reached can be written

$$\alpha = \alpha_{r_{eff}} + \dot{\alpha}t \tag{C5}$$

Substituting this expression for angle of attack in equation (C3) results in

$$\left(\frac{\partial a}{\partial \alpha}\right)_t = K\left[k + m\left(\alpha_{r_{eff}} + \dot{\alpha}t\right)\right]_s \tag{C6}$$

A substitution of this expression for $\left(\frac{\partial a}{\partial \alpha}\right)_t$ in equation (C1) results in

$$\left(\frac{da}{dt}\right)_t = K\dot{\alpha}\left[k + m\left(\alpha_{r_{eff}} + \dot{\alpha}t\right)\right]_s \tag{C7}$$

By integrating over the effective rotation time, $\Delta t_{r_{eff}}$,

$$\Delta a = \int_0^{\Delta t_{r_{eff}}} \frac{da}{dt}\, dt = K\dot{\alpha} \int_0^{\Delta t_{r_{eff}}} \left[k + m\left(\alpha_{r_{eff}} + \dot{\alpha}t\right)\right]_s dt \tag{C8}$$

Thus,

$$a_t = K\dot{\alpha}\left[\left(k + m\alpha_{r_{eff}}\right)_s \Delta t_{r_{eff}} + \frac{\dot{\alpha}\left(\Delta t_{r_{eff}}\right)^2}{2}\right] \tag{C9}$$

Integrating again to obtain the velocity increment,

$$\left(\Delta V_{r_a}\right)_t = K\dot{\alpha}\left[\left(k + m\alpha_{r_{eff}}\right)_s \frac{\left(\Delta t_{r_{eff}}\right)^2}{2} + \frac{\dot{\alpha}\left(\Delta t_{r_{eff}}\right)^3}{6}\right] \tag{C10}$$

One more integration results in the ground roll increment

$$\left(\Delta S_{r_a}\right)_t = K\dot{\alpha}\left[\left(k + m\alpha_{r_{eff}}\right)_s \frac{\left(\Delta t_{r_{eff}}\right)^3}{6} + \frac{\dot{\alpha}\left(\Delta t_{r_{eff}}\right)^4}{24}\right] \tag{C11}$$

APPENDIX D

PROCEDURES FOR EVALUATING ROTATION METHODS

Verification of ΔV_{r_a} and ΔS_{r_a}

The losses in velocity and distance during rotation due to the loss of acceleration were calculated directly from the cinetheodolite data and compared with the loss predicted by the methods. That is, the results of the equation

$$\left(\Delta V_{r_a}\right)_t = \left(\Delta V_r\right)_t - \left(a_r \Delta t_r\right)_t$$

were compared with $\left(\Delta V_{r_a}\right)_{p_1}$ and $\left(\Delta V_{r_a}\right)_{p_2}$, and the results of the equation

$$\left(\Delta S_{r_a}\right)_t = \left(\Delta S_r\right)_t - \left(V_r \Delta t_r\right)_t - \left(0.5 a_r \Delta t_r^2\right)_t$$

were compared with $\left(\Delta S_{r_a}\right)_{p_1}$ and $\left(\Delta S_{r_a}\right)_{p_2}$. The actual effective rotation time, $\left(\Delta t_{r_{eff}}\right)_t$, was used to calculate predictions of losses in velocity and distance to avoid errors in Δt_r that might result from using a performance test curve like that shown in figure 9.

Verification of $\left(\Delta V_r\right)_{p_2}$ and $\left(\Delta S_r\right)_{p_2}$

The term Δt_r was evaluated (see fig. 9) by using values of $\left(V_{lof}\right)_t$ and $\dot{\alpha}$ given by the measurements. With Δt_r and a_r, which was determined from the fairing in figure 8, a prediction was made of the change in velocity during rotation assuming no loss of acceleration. Then the velocity loss during rotation due to acceleration decay, ΔV_{r_a}, was calculated, as follows: An approximate initial rotation velocity, V_r, was calculated from the measured value of $\left(V_{lof}\right)_t$ and the

calculated change in velocity without loss of acceleration. This value, combined with other known quantities, allowed an approximation to be made of ΔV_{r_a} (see eq. (C10)). A more accurate value of V_r was found by subtracting this approximation of ΔV_{r_a} from the approximate value of V_r. The term ΔV_{r_a} was recalculated using this new value of V_r. This value of ΔV_{r_a} was used to make the final prediction of rotation velocity:

$$\left(V_r\right)_{p_2} = \left(V_{lof}\right)_t - \left(a_r \Delta t_r\right)_{p_2} - \left(\Delta V_{r_a}\right)_{p_2} \tag{D1}$$

Once $\left(V_r\right)_{p_2}$ was determined, ΔS_{r_a} could be calculated by using equation (C11), and $\left(S_r\right)_{p_2}$ could be calculated from $\left(S_{lof}\right)_t$. Finally, $\left(\Delta V_r\right)_{p_2}$ and $\left(\Delta S_r\right)_{p_2}$ were calculated, as follows:

$$\left(\Delta V_r\right)_{p_2} = \left(V_{lof}\right)_t - \left(V_r\right)_{p_2} \tag{D2}$$

$$\left(\Delta S_r\right)_{p_2} = \left(S_g\right)_t - \left(S_r\right)_{p_2} \tag{D3}$$

REFERENCES

1. Larson, Terry J.; and Schweikhard, William G.: Verification of Takeoff Performance Predictions for the XB-70 Airplane. NASA TM X-2215, 1971.

2. Lush, Kenneth J.: Standardization of Take-Off Performance Measurements for Airplanes. Tech. Note R-12, Air Force Flight Test Center, U.S. Air Force.

3. Mechtly, E. A.: The International System of Units. Physical Constants and Conversion Factors. Second Revision. NASA SP-7012, 1973.

4. Wolowicz, Chester H.: Analysis of an Emergency Deceleration and Descent of the XB-70-1 Airplane Due to Engine Damage Resulting From Structural Failure. NASA TM X-1195, 1966.

5. Bowman, Paul V.: Estimated Performance Report for the XB-70A Air Vehicle No. 2. Rep. No. NA-65-661, North American Aviation, Inc., July 26, 1965.

6. Hall, Albert W.: Take-Off Distances of a Supersonic Transport Configuration as Affected by Airplane Rotation During the Take-Off Run. NASA TN D-982, 1961.

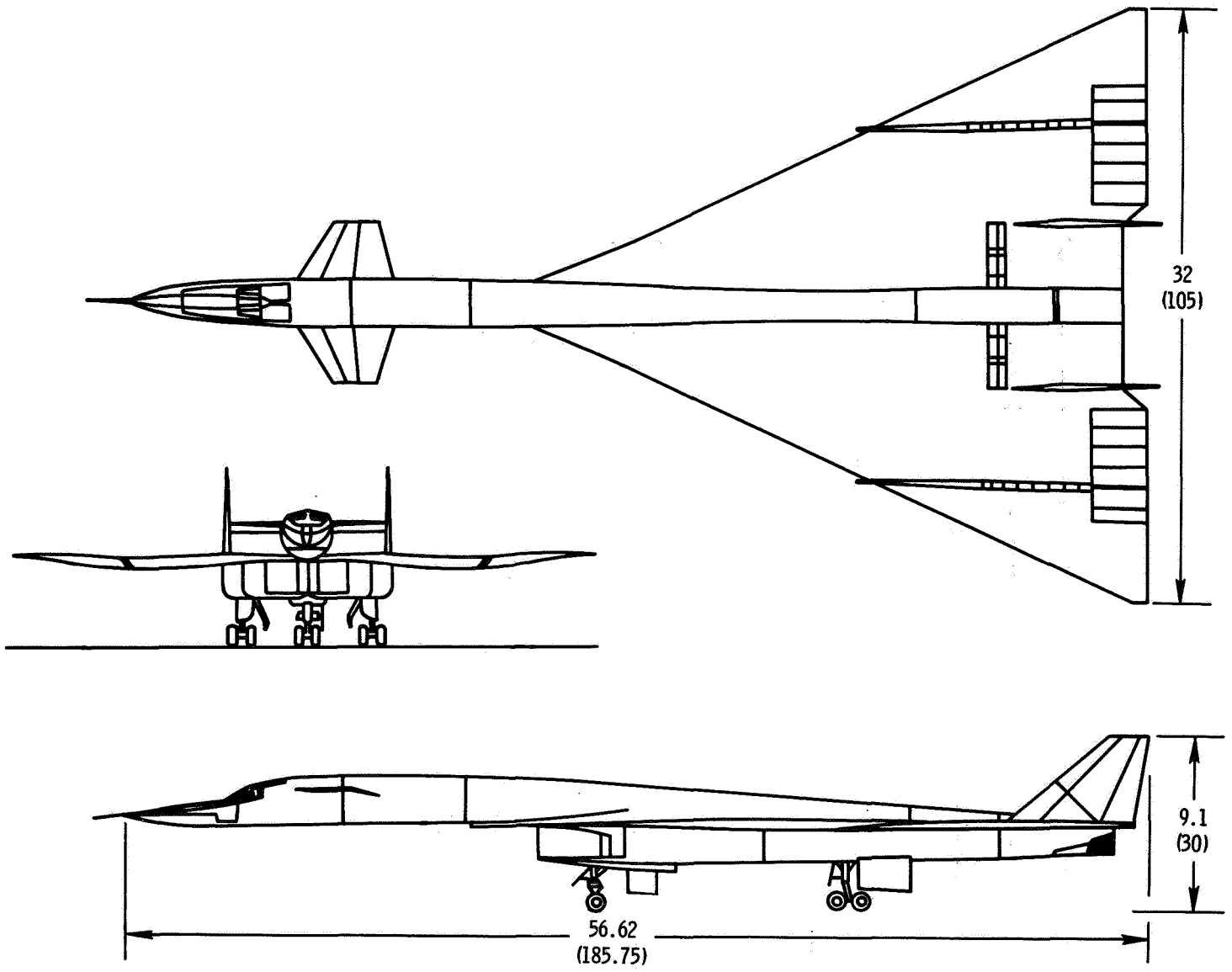

Figure 1. Three-view drawing of the XB-70 airplane. Dimensions in meters (feet).

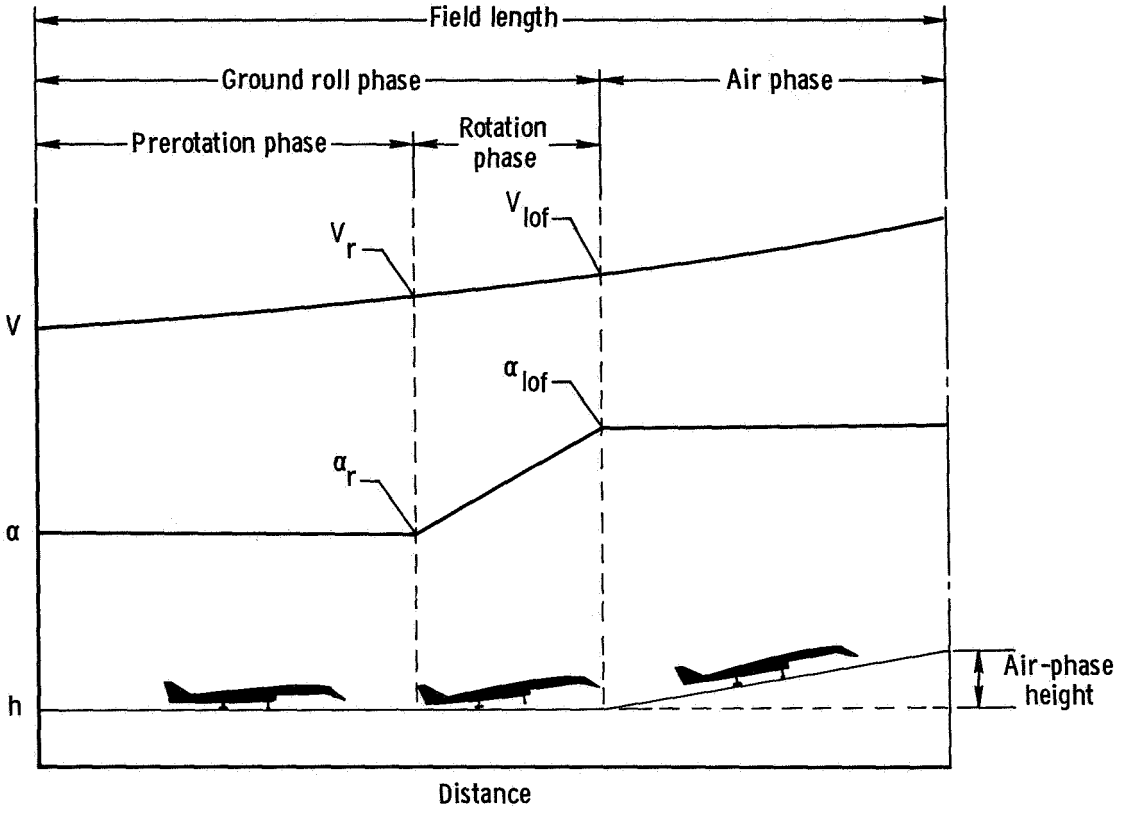

Figure 2. Takeoff phases.

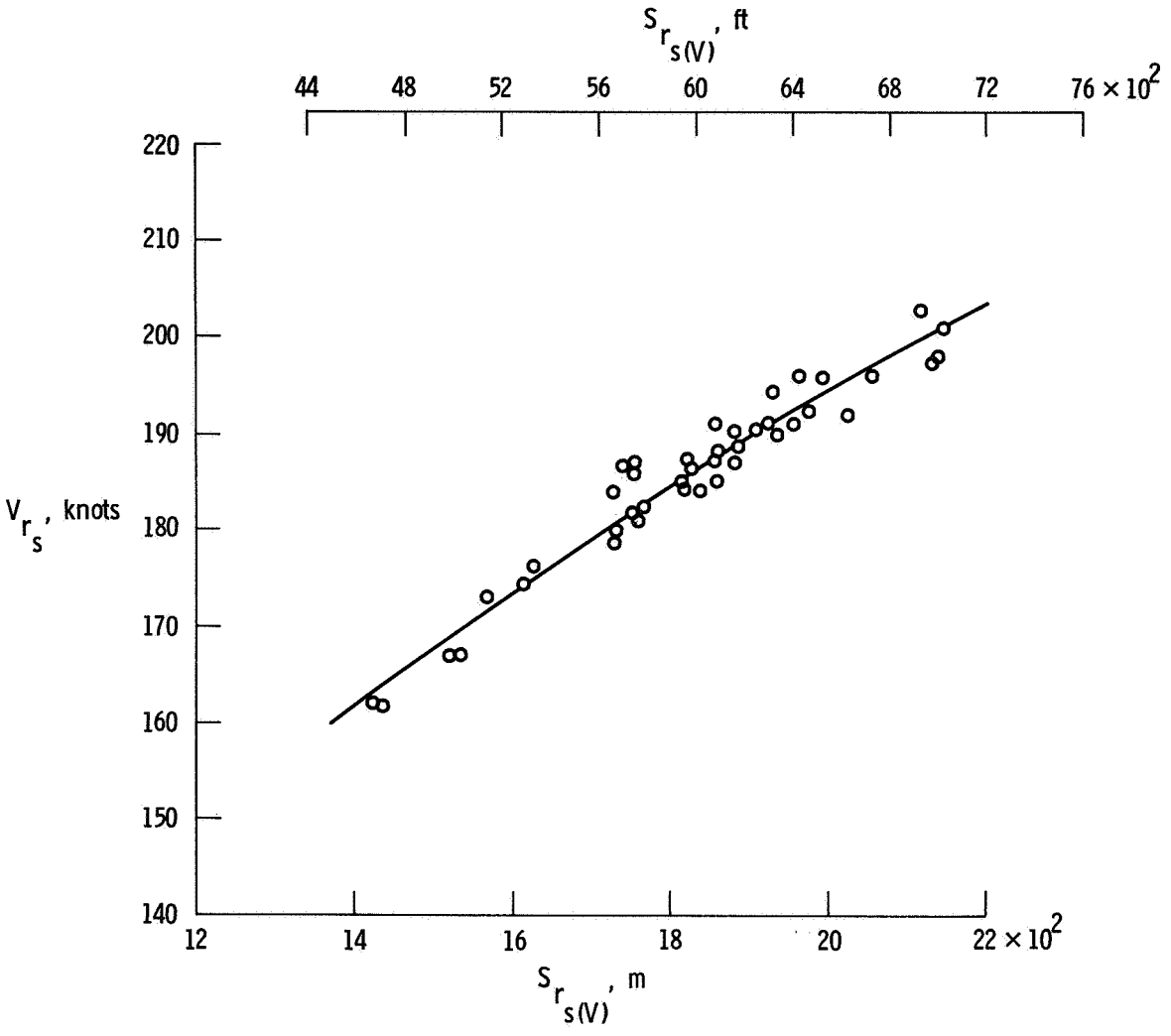

Figure 3. Variation with velocity of ground roll distance at beginning of rotation. Data from reference 1. W_s = 2313 kilonewtons (520,000 pounds force).

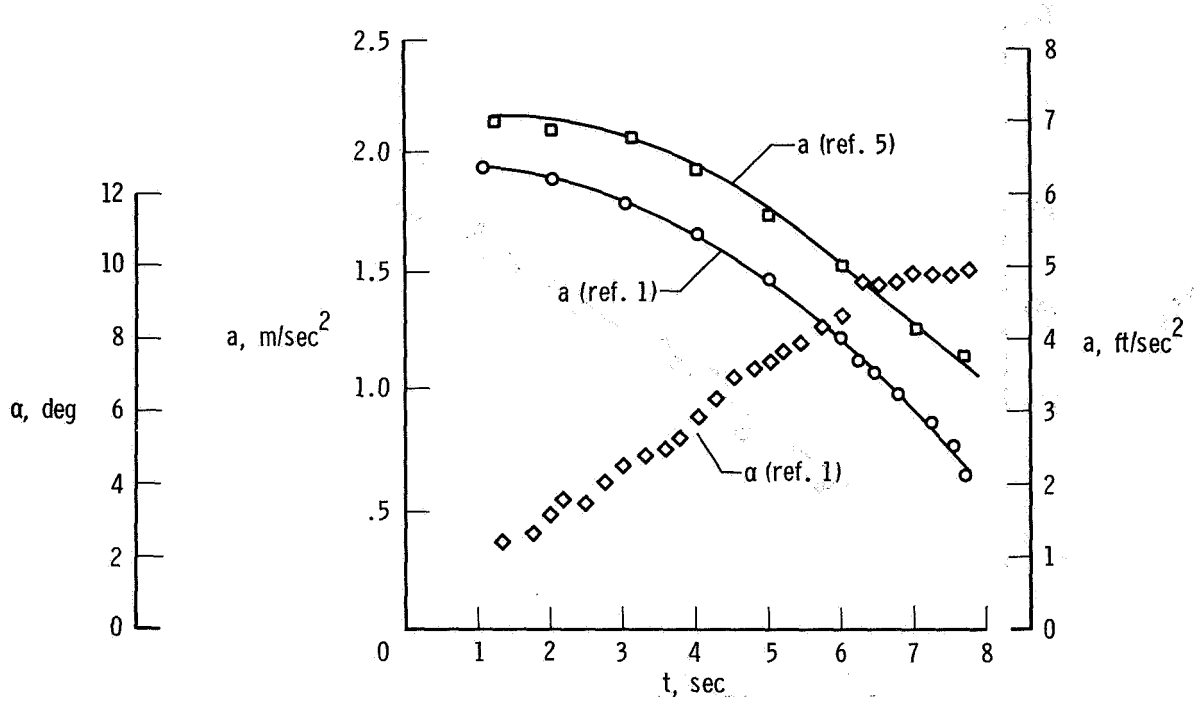

Figure 4. Time histories of acceleration and angle of attack for a typical rotation during ground roll.

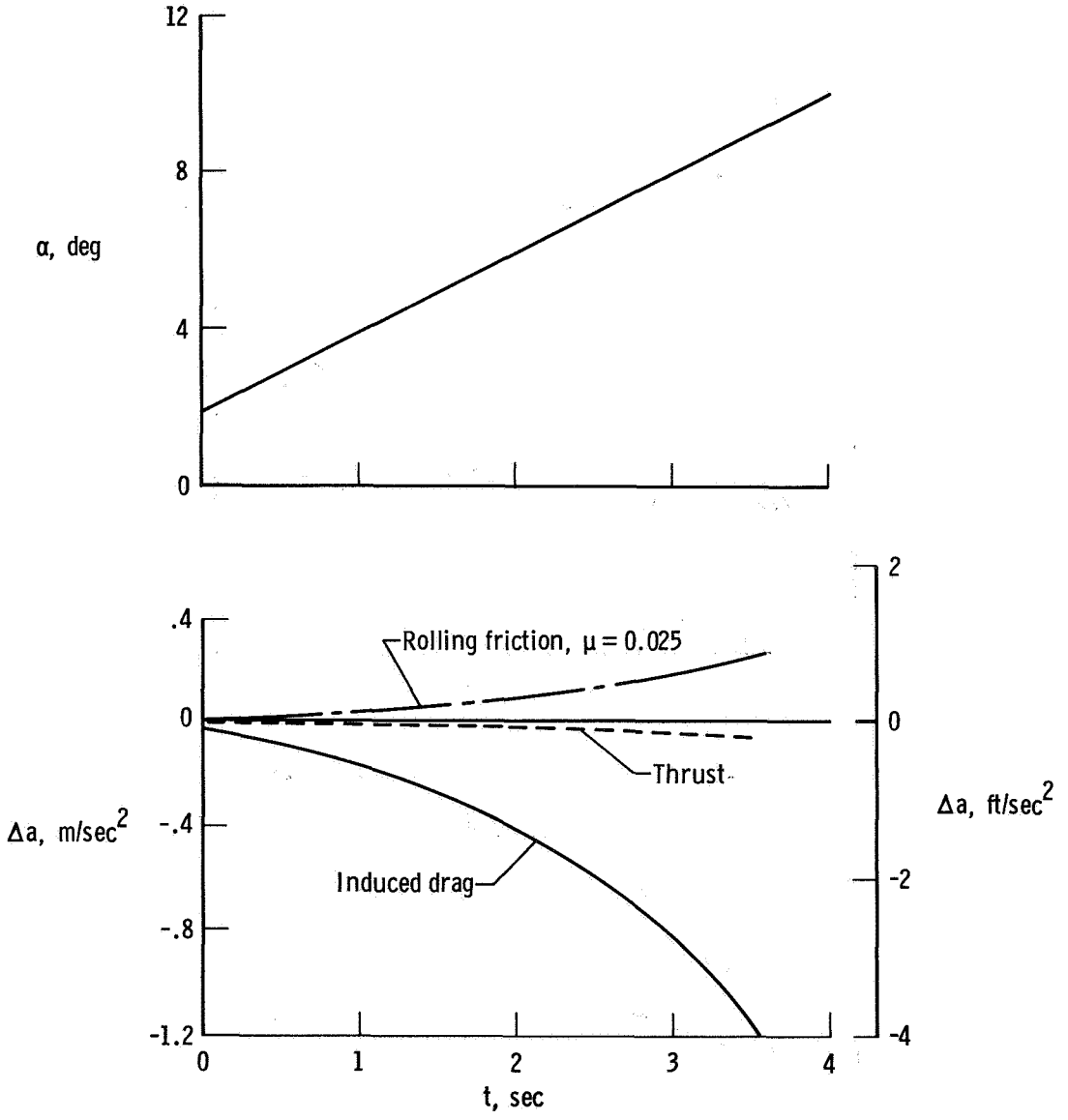

Figure 5. Change in acceleration during rotation phase of takeoff due to induced drag, thrust, and rolling friction. W_r = 2313 kilonewtons (520,000 pounds force); F_{n_r} = 689.47 kilonewtons (155,000 pounds force); ρ = 1.225 kg/m^3 (0.002377 slug/ft^3).

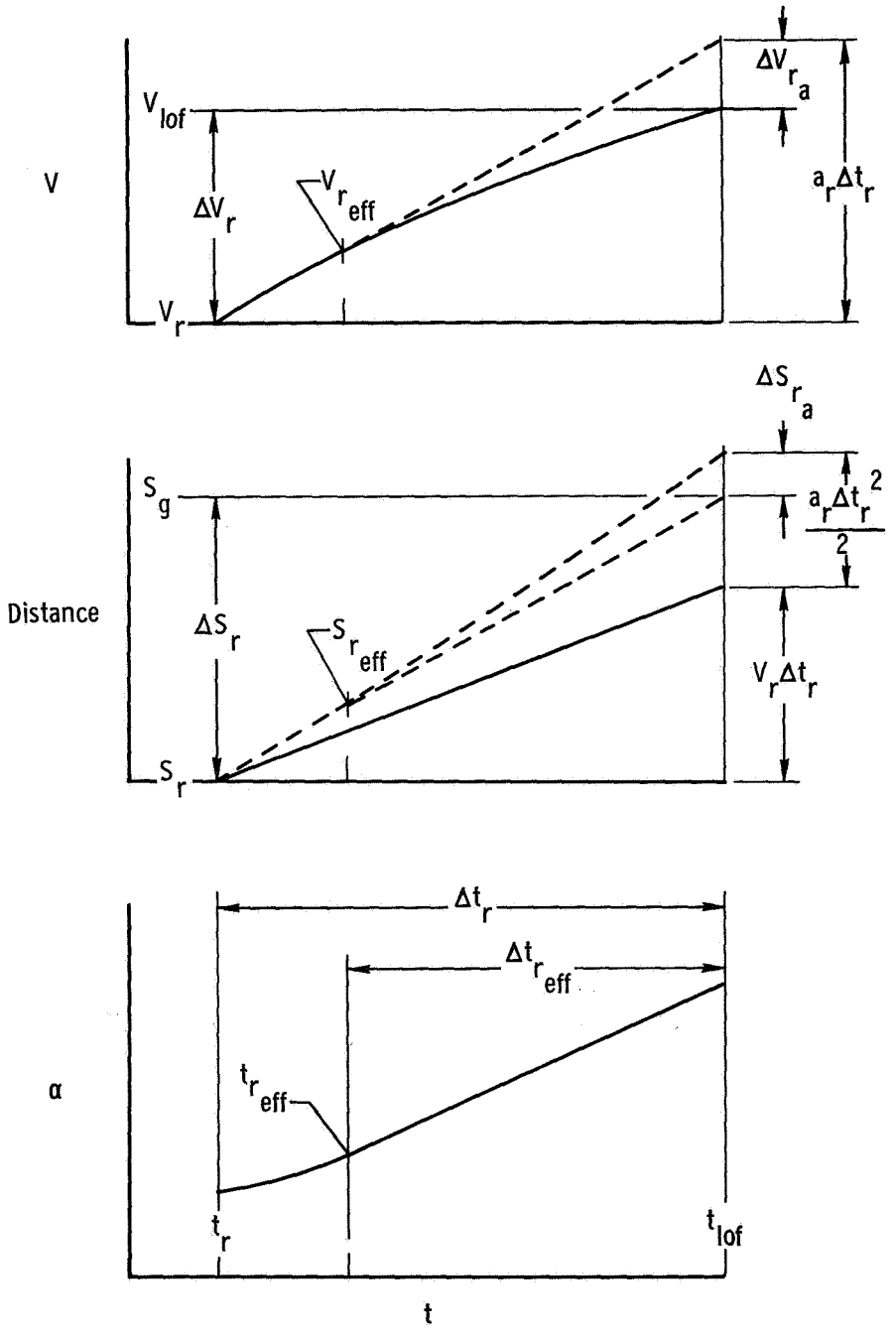

Figure 6. Rotation phase quantities.

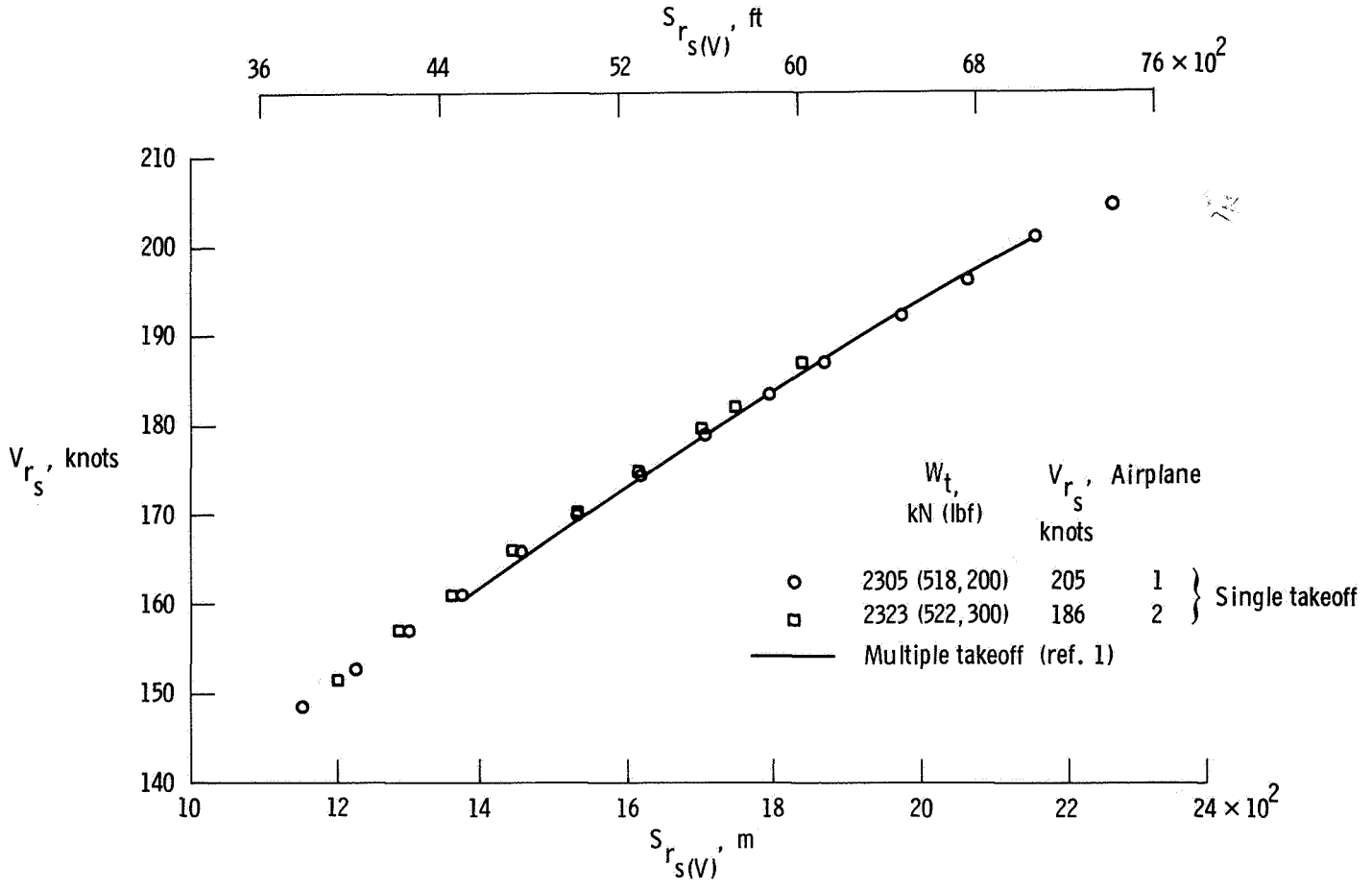

Figure 7. Variation with velocity of ground roll distance at beginning of rotation. W_s = 2313 kilonewtons (520,000 pounds force).

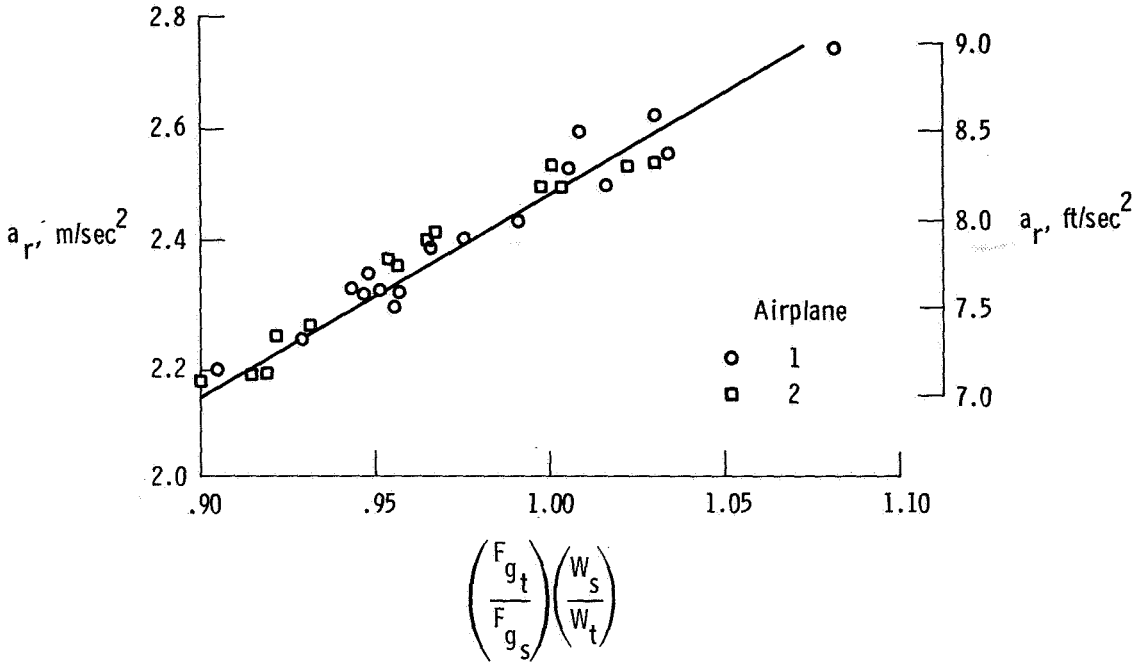

Figure 8. Acceleration at beginning of rotation as a function of test quantities.

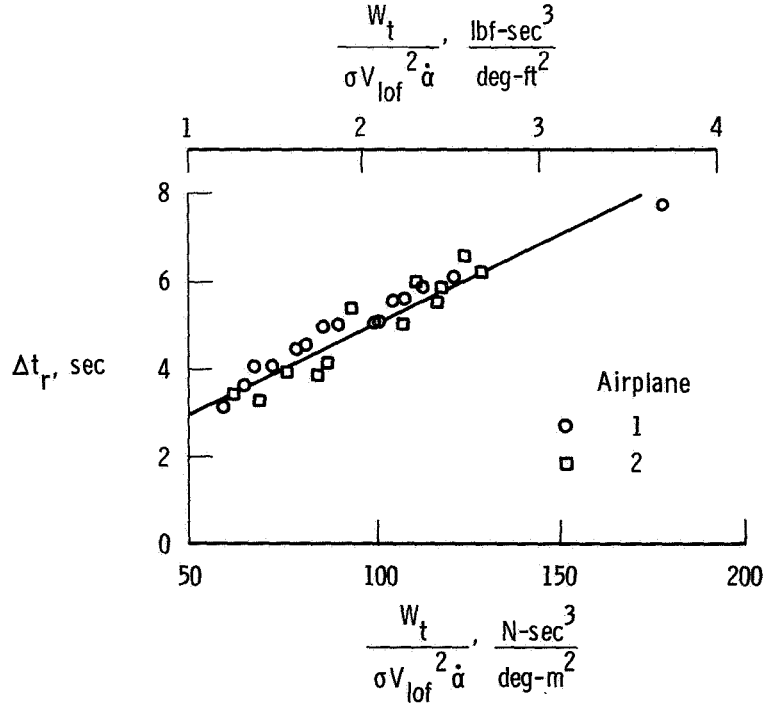

Figure 9. Time from beginning of rotation to lift-off as a function of test quantities.

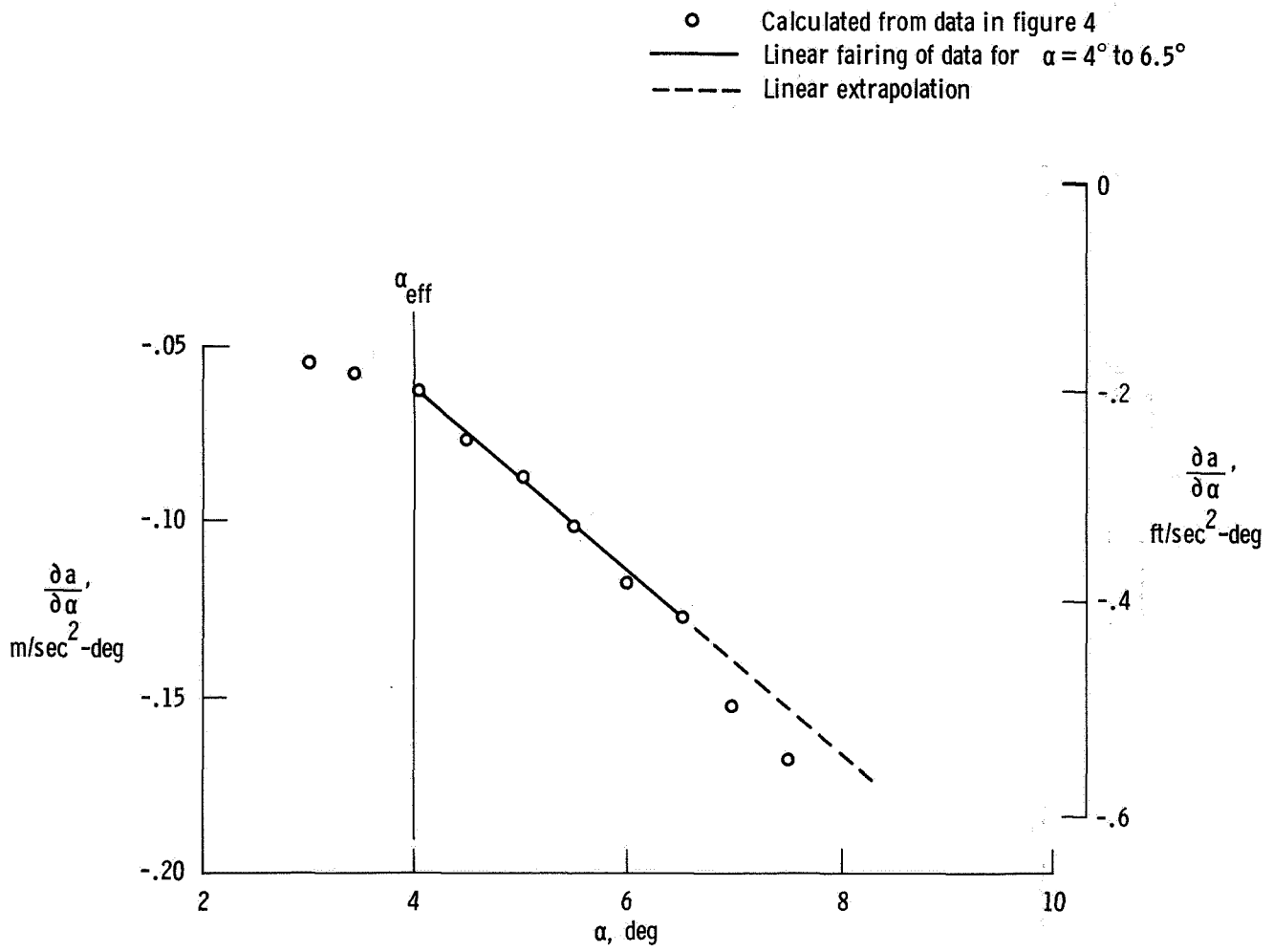

Figure 10. Partial derivative of acceleration with respect to angle of attack as a function of angle of attack. Calculated from data in figure 4.

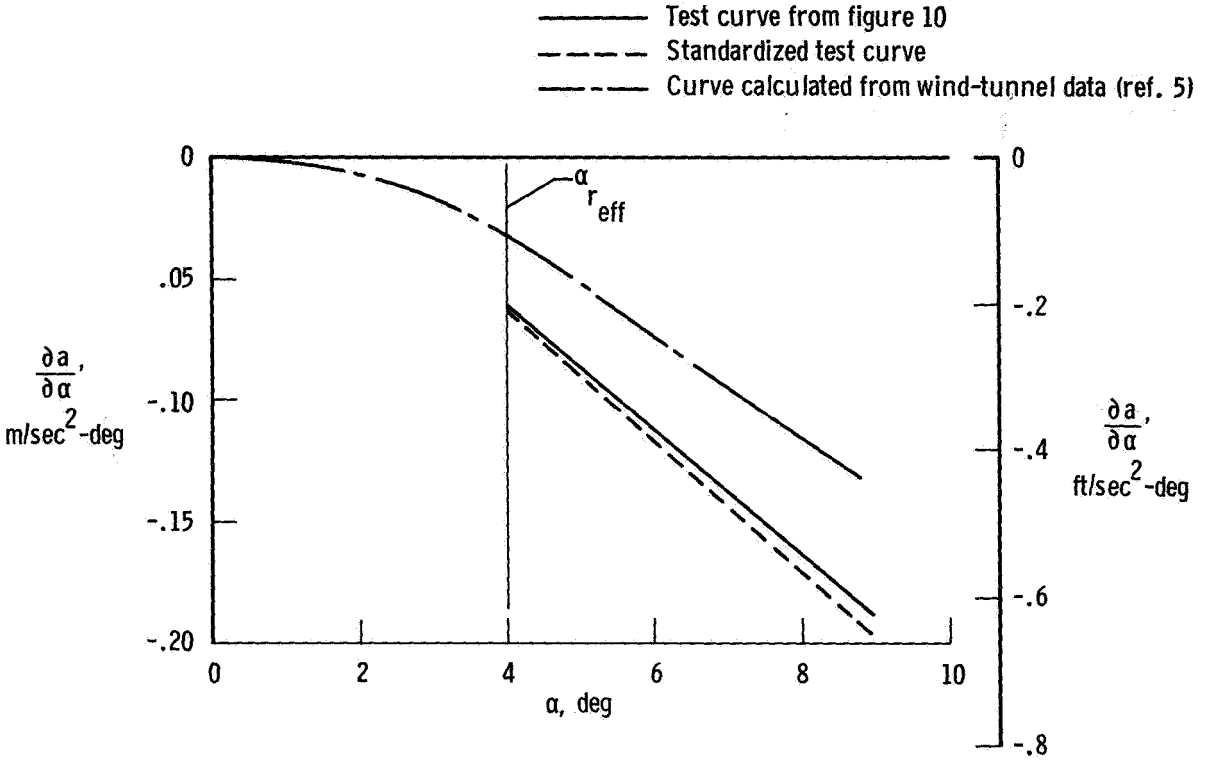

Figure 11. Experimentally and analytically derived curves of $\frac{\partial a}{\partial \alpha}$ as a function of angle of attack.

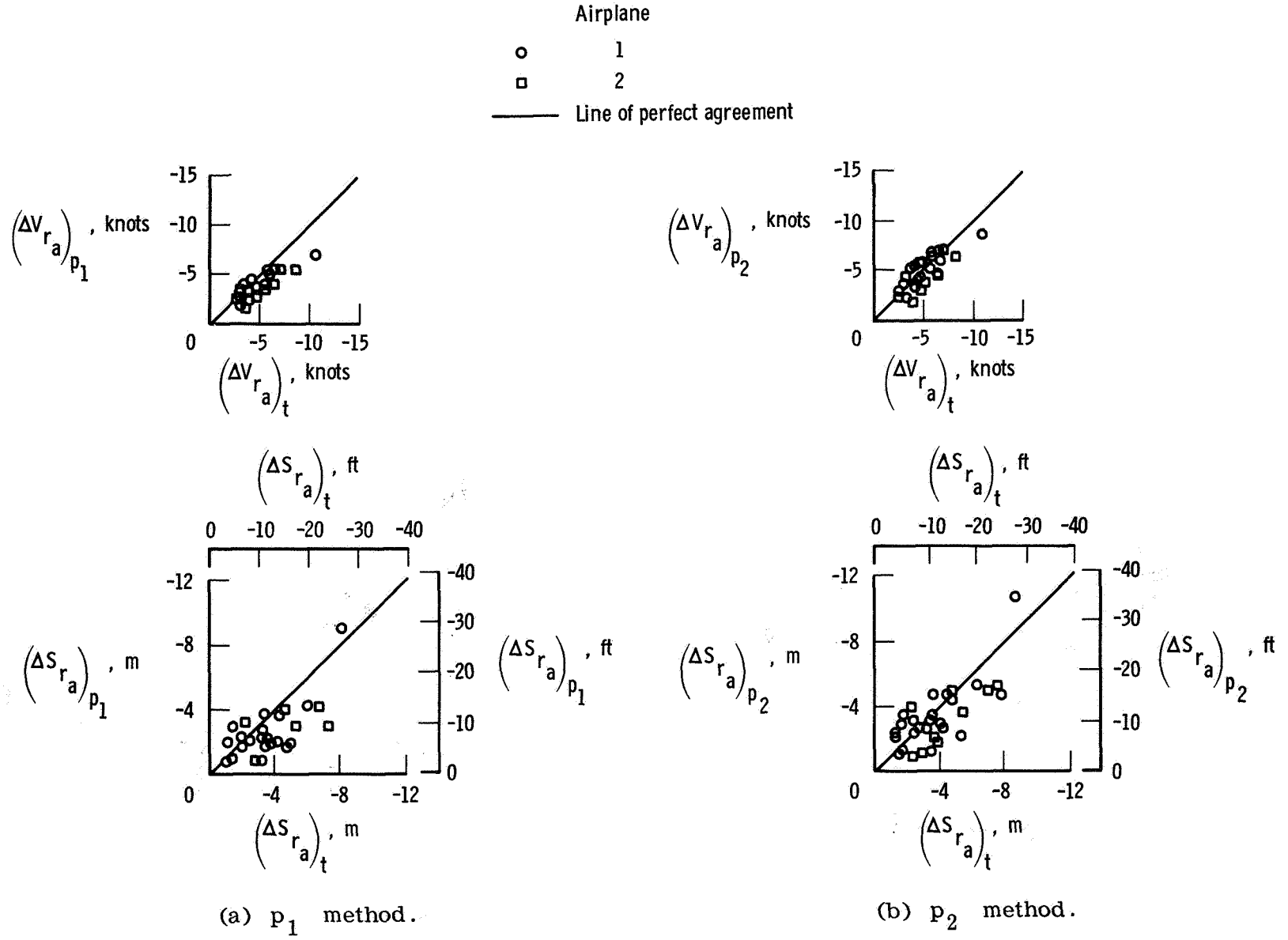

(a) p_1 method.

(b) p_2 method.

Figure 12. Comparison of predicted and experimental change in velocity and distance during rotation due to change in acceleration.

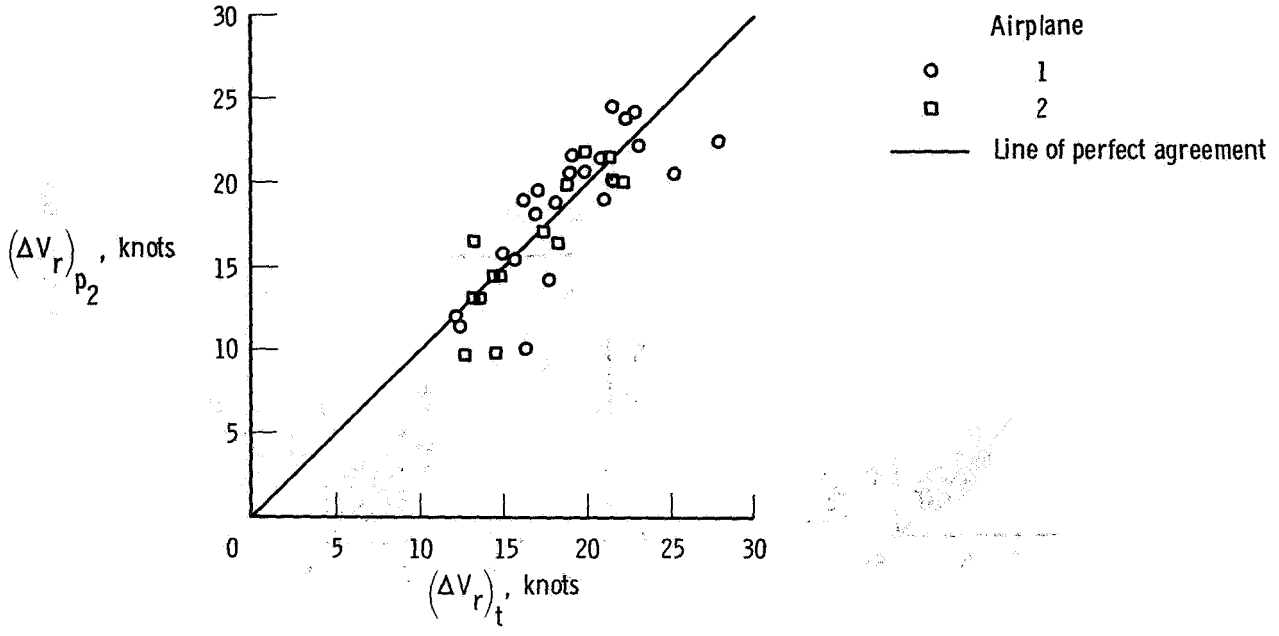

(a) Rotation velocity increment.

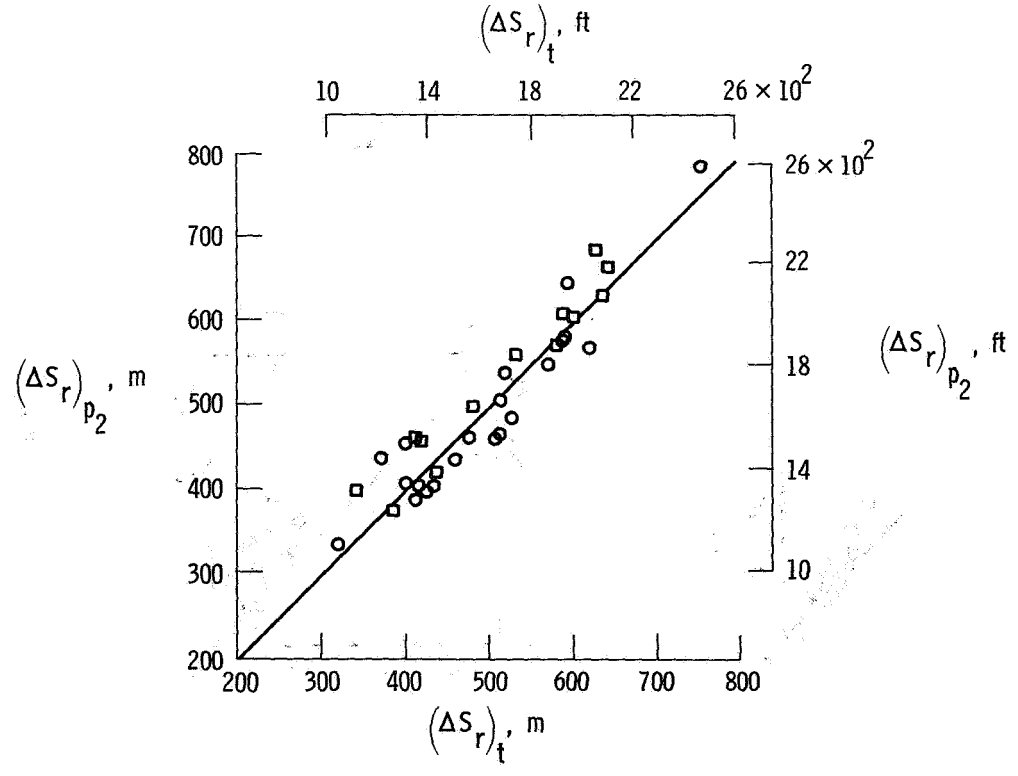

(b) Rotation distance increment.

Figure 13. Comparison of predicted and experimental change in total velocity and distance during rotation.

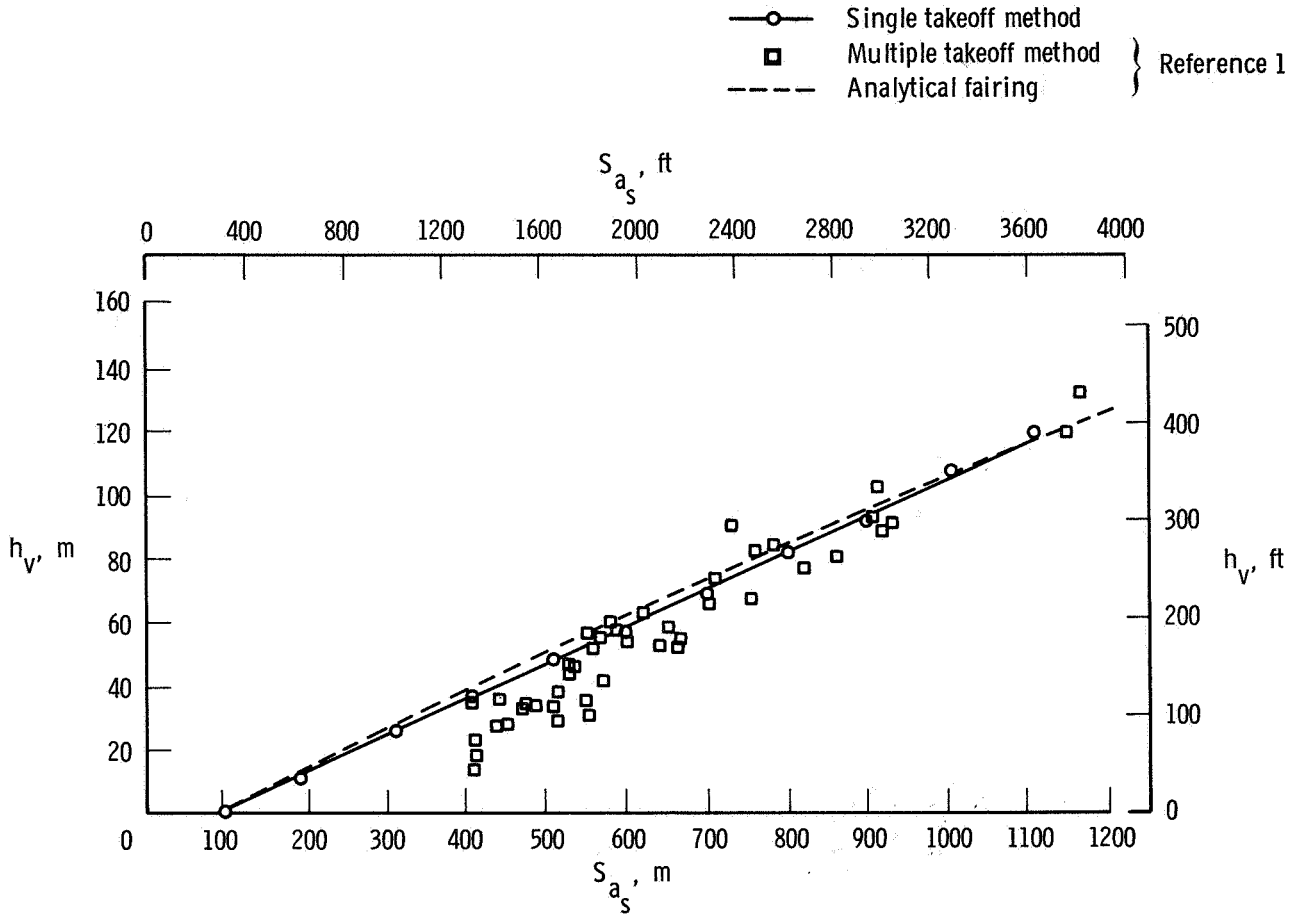

Figure 14. Variation of kinetic energy gain with air-phase distance to a height of 10.7 meters (35 feet). W_s = 2313 kilonewtons (520,000 pounds force).

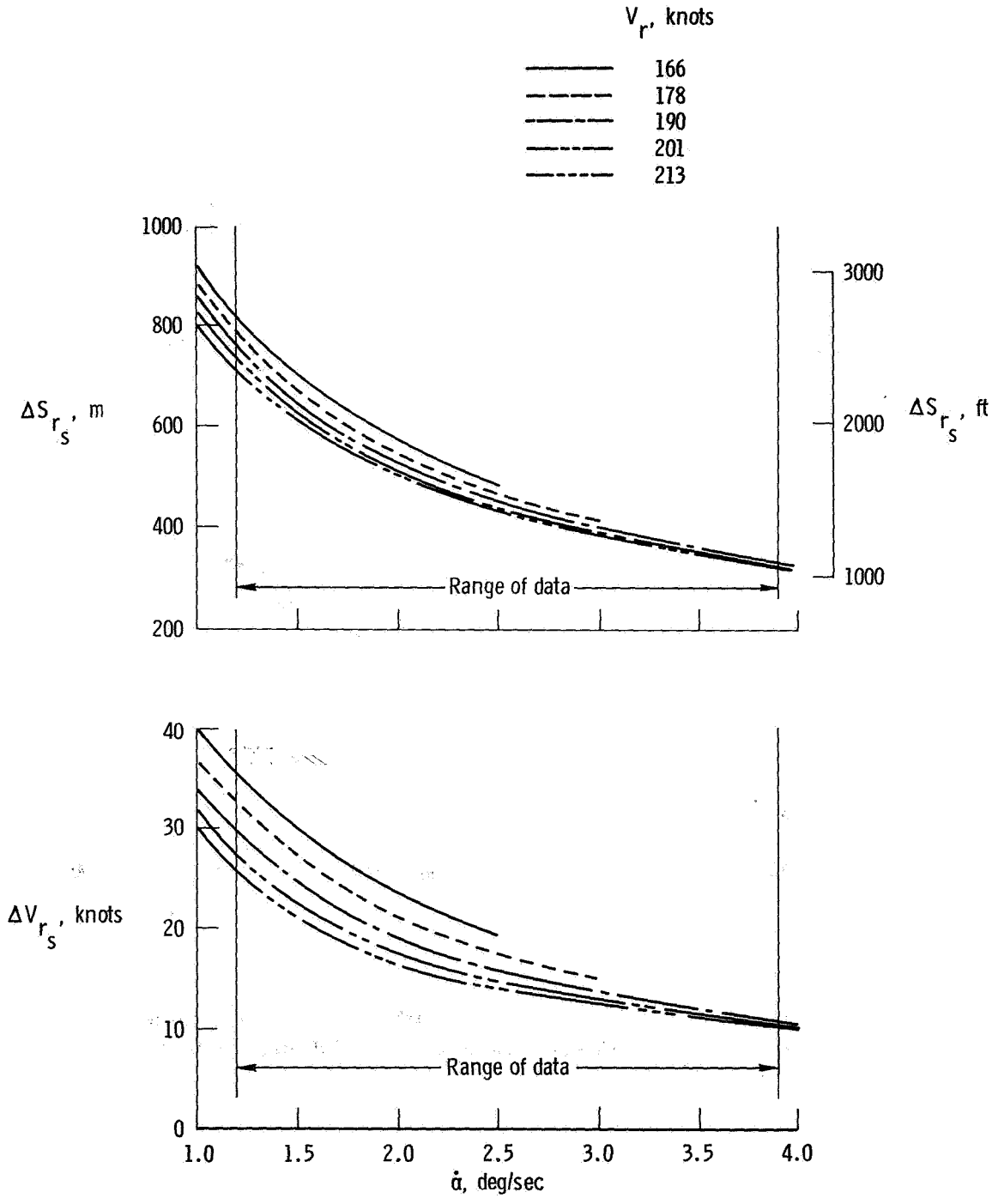

Figure 15. Effect of rotation initiation velocity and rotation rate on velocity and distance increments during rotation phase. W_s = 2313 kilonewtons (520,000 pounds force); standard sea-level conditions.

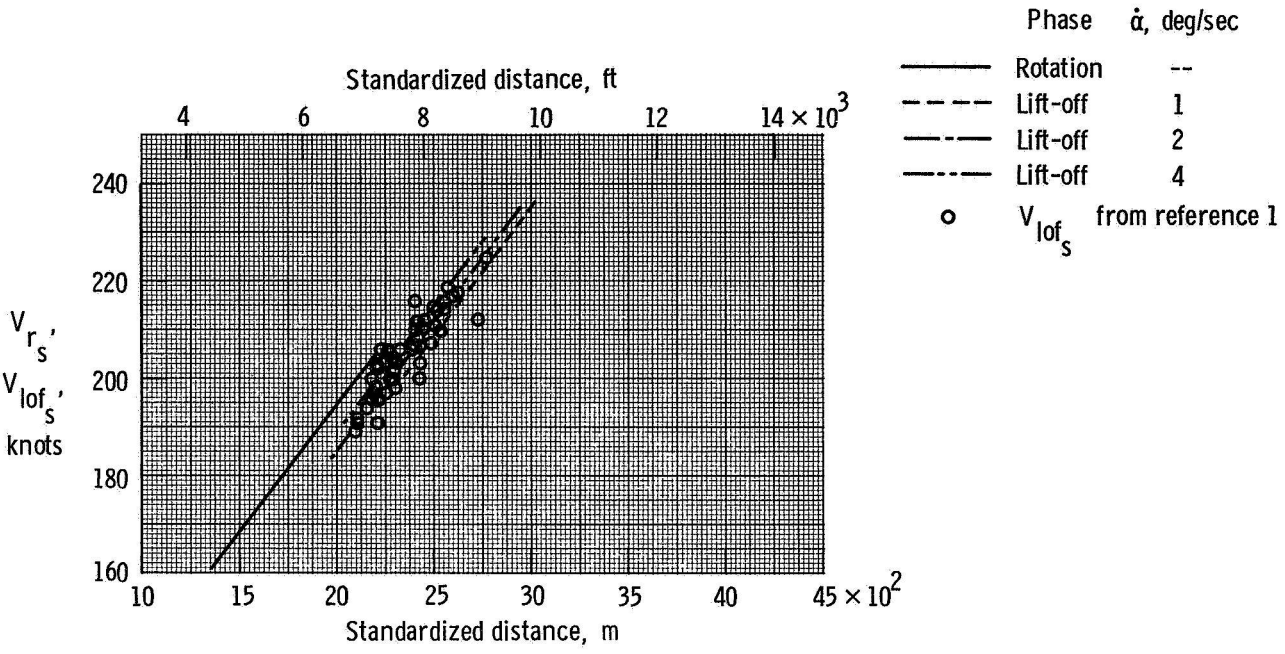

(a) Ground roll performance.

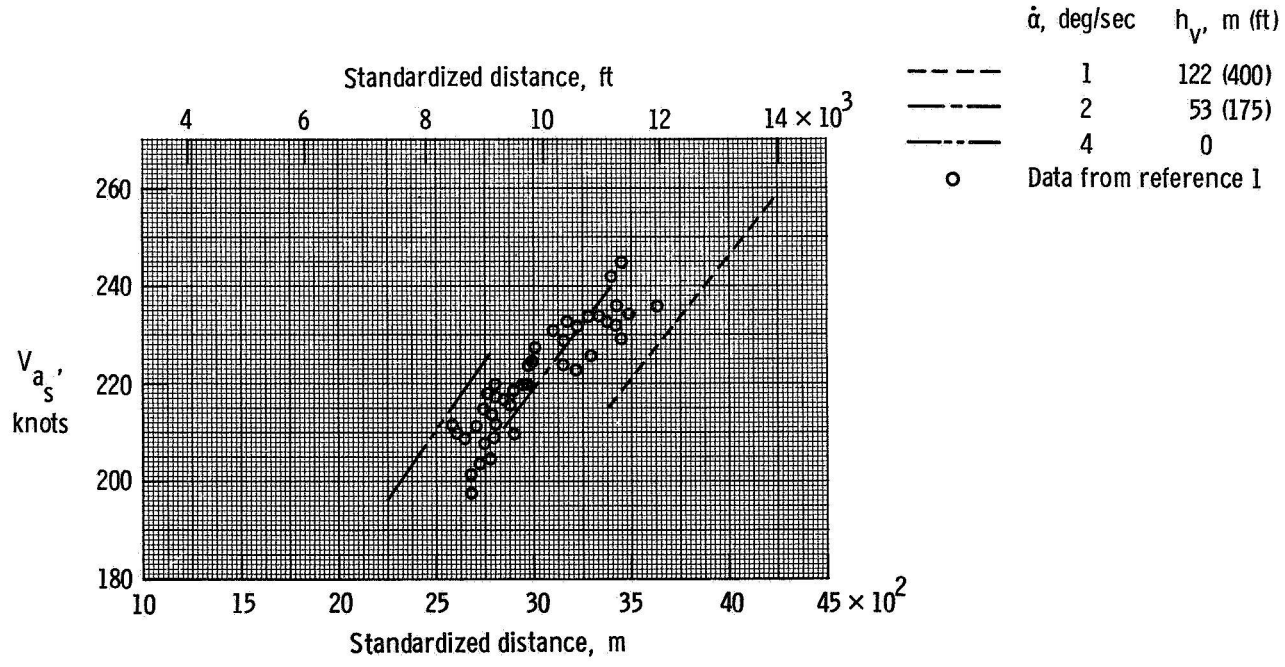

(b) Field length performance.

Figure 16. Standardized takeoff performance envelope as calculated from results of proposed method and standardized takeoff data from reference 1. W_s = 2313 kilonewtons (520,000 pounds force).

"The aeronautical and space activities of the United States shall be conducted so as to contribute . . . to the expansion of human knowledge of phenomena in the atmosphere and space. The Administration shall provide for the widest practicable and appropriate dissemination of information concerning its activities and the results thereof."

—NATIONAL AERONAUTICS AND SPACE ACT OF 1958

NASA SCIENTIFIC AND TECHNICAL PUBLICATIONS

TECHNICAL REPORTS: Scientific and technical information considered important, complete, and a lasting contribution to existing knowledge.

TECHNICAL NOTES: Information less broad in scope but nevertheless of importance as a contribution to existing knowledge.

TECHNICAL MEMORANDUMS: Information receiving limited distribution because of preliminary data, security classification, or other reasons. Also includes conference proceedings with either limited or unlimited distribution.

CONTRACTOR REPORTS: Scientific and technical information generated under a NASA contract or grant and considered an important contribution to existing knowledge.

TECHNICAL TRANSLATIONS: Information published in a foreign language considered to merit NASA distribution in English.

SPECIAL PUBLICATIONS: Information derived from or of value to NASA activities. Publications include final reports of major projects, monographs, data compilations, handbooks, sourcebooks, and special bibliographies.

TECHNOLOGY UTILIZATION PUBLICATIONS: Information on technology used by NASA that may be of particular interest in commercial and other non-aerospace applications. Publications include Tech Briefs, Technology Utilization Reports and Technology Surveys.

Details on the availability of these publications may be obtained from:

SCIENTIFIC AND TECHNICAL INFORMATION OFFICE

NATIONAL AERONAUTICS AND SPACE ADMINISTRATION

Washington, D.C. 20546